

Equation of State for Nucleonic Matter and its Quark Mass Dependence from the Nuclear Force in Lattice QCD

Takashi Inoue¹, Sinya Aoki^{2,3}, Takumi Doi⁴, Tetsuo Hatsuda^{4,5},
Yoichi Ikeda⁴, Noriyoshi Ishii³, Keiko Murano⁴, Hidekatsu Nemura³, Kenji Sasaki³

(HAL QCD Collaboration)

¹*Nihon University, College of Bioresource Sciences, Kanagawa 252-0880, Japan*

²*Yukawa Institute for Theoretical Physics, Kyoto University, Kyoto 606-8502, Japan*

³*Center for Computational Sciences, University of Tsukuba, Ibaraki 305-8571, Japan*

⁴*Theoretical Research Division, Nishina Center, RIKEN, Saitama 351-0198, Japan*

⁵*Kavli IPMU (WPI), The University of Tokyo, Chiba 277-8583, Japan*

Quark mass dependence of the equation of state (EOS) for nucleonic matter is investigated, on the basis of the Brueckner-Hartree-Fock method with the nucleon-nucleon interaction extracted from lattice QCD simulations. We observe saturation of nuclear matter at the lightest available quark mass corresponding to the pseudoscalar meson mass $\simeq 469$ MeV. Mass-radius relation of the neutron stars is also studied with the EOS for neutron-star matter from the same nuclear force in lattice QCD. We observe that the EOS becomes stiffer and thus the maximum mass of neutron star increases as the quark mass decreases toward the physical point.

PACS numbers: 12.38.Gc, 13.75.Cs, 21.65.Mn, 26.60.Kp

The equation of state (EOS) for hadronic matter is a key quantity for understanding the physics of compact stars and explosive phenomena in astrophysics. From the observational point of view, recent reports on massive neutron stars put stringent constraints on the EOS [1]. In the future, neutrinos from core-collapsed supernovae and gravitational waves from neutron star mergers will give further constraints on the EOS [2, 3]. From the theoretical point of view, various approaches to calculate the EOS have been pursued so far, e.g. the Brueckner-Bethe-Goldstone theory [4], the quantum Monte Carlo simulations [5], and the chiral effective theories [6, 7]. Although they provide reasonable descriptions of the nuclear matter at low density, it is still beyond the scope of these approaches to answer the fundamental questions such as the quark-mass (m_q) dependence of the nuclear saturation property and the maximum mass of neutron stars. These questions can only be answered by many-body techniques with hadronic interactions obtained by lattice QCD simulations for different m_q .

The purpose of this Letter is to make a first exploratory study for the nuclear and neutron matter EOS by combining the Brueckner-Hartree-Fock (BHF) many-body theory with the nuclear force obtained from lattice QCD simulations. In particular we study how the saturation develops in nuclear matter and how the mass-radius relation of the neutron star changes as a function of m_q : Such m_q dependence of the EOS gives us useful information on the physics of strongly interacting nucleons, even though the values of m_q in this study are still away from the physical one. In addition, it is certainly important to establish a direct connection between lattice QCD and the physics of the nucleonic matter.

The nuclear force which we adopt in this Letter is taken from the zero-strangeness sector of the octet-

TABLE I: M_{PS} , M_{V} and M_{B} denote hadron masses corresponding to the pseudoscalar meson, vector meson and octet baryon, respectively, with the $SU(3)$ symmetric hopping parameter κ_{uds} [9]. Trajectory length N_{traj} and number of configurations N_{cfg} are also shown.

κ_{uds}	M_{PS} [MeV]	M_{V} [MeV]	M_{B} [MeV]	$N_{\text{cfg}} / N_{\text{traj}}$
0.13660	1170.9(7)	1510.4(0.9)	2274(2)	420 / 4200
0.13710	1015.2(6)	1360.6(1.1)	2031(2)	360 / 3600
0.13760	836.5(5)	1188.9(0.9)	1749(1)	480 / 4800
0.13800	672.3(6)	1027.6(1.0)	1484(2)	360 / 3600
0.13840	468.6(7)	829.2(1.5)	1161(2)	720 / 3600

baryon potentials in the flavor- $SU(3)$ limit calculated on the lattice [8, 9], where the renormalization group improved Iwasaki gauge action and the nonperturbatively improved Wilson quark action were employed on a $32^3 \times 32$ lattice with the lattice spacing $a = 0.121(2)$ fm. The potentials were derived from the imaginary-time Nambu-Bethe-Salpeter wave functions by the HAL QCD method [10–12], at the quark masses corresponding to the pseudoscalar meson masses (M_{PS}) ranging between 469 and 1171 MeV. Shown together in Table I are the vector meson mass (M_{V}) and the baryon mass (M_{B}) for these quark masses.

In Fig. 1, we show the NN potentials obtained from fits to the lattice data in S and D-waves at $M_{\text{PS}} \simeq 469$ MeV. These potentials share common features with phenomenological potentials, i.e., a strong repulsive core at short distance and the attractive pocket at intermediate distance, so that the 1S_0 phase shift in Fig. 2 shows qualitatively similar behavior with the experimental data [9]. While the phase shift in the 3S_1 channel shows stronger attraction at low energies than that of the

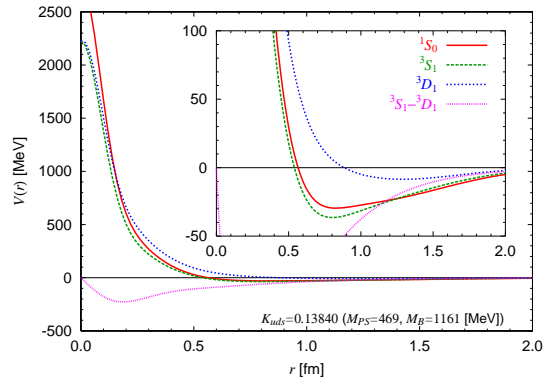


FIG. 1: The NN potentials for S and D waves extracted from lattice QCD data at $M_{PS} = 469$ MeV in the flavor- $SU(3)$ limit. The lines are obtained by the least χ^2 fit to the lattice data (see [9] for the fit function).

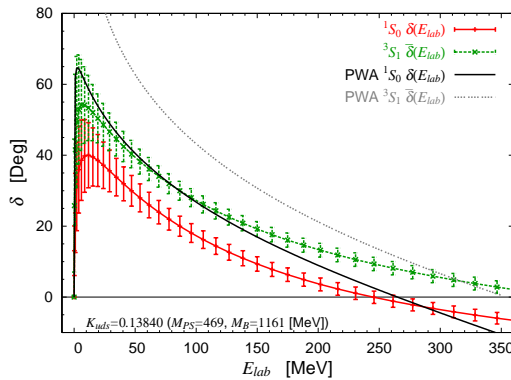


FIG. 2: Phases shifts of NN scattering as a function of energy in the laboratory frame, extracted from lattice QCD data at $M_{PS} = 469$ MeV in the flavor- $SU(3)$ limit: The black and gray dashed lines are partial wave analysis (PWA) of experimental data taken from NN-Online (<http://nn-online.org/>).

1S_0 channel due to 3S_1 - 3D_1 mixing, it is still insufficient to form the deuteron bound state even at $M_{PS} \simeq 469$ MeV [9, 13]. Although we found no bound state in two and three nucleon systems, there exists a four-nucleon bound state, namely, ^4He , with about 5 MeV binding energy at $M_{PS} \simeq 469$ MeV [9].

Let us now study the EOS for nuclear matter and neutron matter in the leading order of the Brueckner-Bethe-Goldstone (BBG) hole-line expansion, i.e., the Brueckner-Hartree-Fock (BHF) theory (see e.g. [4]), where the total ground-state energy E at zero temperature with the nucleon mass M_N and the Fermi momentum k_F reads

$$E = \sum_k^{k_F} \frac{k^2}{2M_N} + \frac{1}{2} \sum_{k,k'}^{k_F} \text{Re} \langle kk' | G(e(k) + e(k')) | kk' \rangle_A \quad (1)$$

with $|kk'\rangle_A \equiv |kk'\rangle - |k'k\rangle$. To simplify the notation, spin and isospin indices of the nucleons are included in

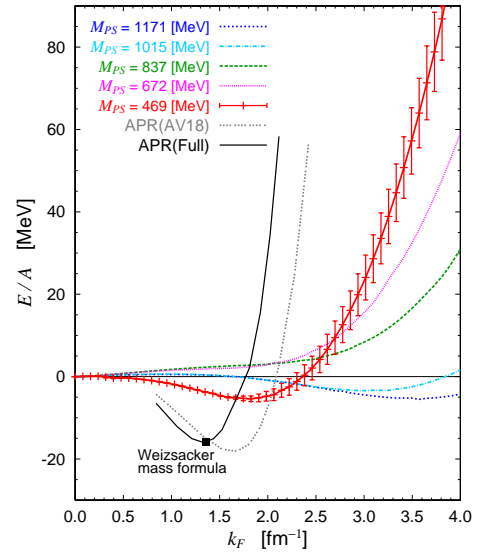


FIG. 3: Ground state energy per nucleon (E/A) for symmetric nuclear matter as a function of k_F obtained by the BHF theory with the NN potential from lattice QCD. Filled square indicates the empirical saturation point, and the curves labeled APR are taken from Ref. [16] with and without the phenomenological three nucleon force. The error bars for the result at $M_{PS} \simeq 469$ MeV are the statistical uncertainties estimated by dividing the gauge configurations into two sets.

the label k . The G matrix, describing the in-medium effective interaction of the two nucleons, obeys the Bethe-Goldstone integral equation with the bare interaction V ,

$$\langle k_1 k_2 | G(\omega) | k_3 k_4 \rangle = \langle k_1 k_2 | V | k_3 k_4 \rangle + \sum_{k_5, k_6} \frac{\langle k_1 k_2 | V | k_5 k_6 \rangle Q(k_5, k_6) \langle k_5 k_6 | G(\omega) | k_3 k_4 \rangle}{\omega - e(k_5) - e(k_6)} \quad (2)$$

where $Q(k, k') = \theta(k - k_F)\theta(k' - k_F)$ is the Pauli exclusion operator to prevent two nucleons from scattering into occupied states. The single particle energy $e(k) = \frac{k^2}{2M_N} + U(k)$ contains the single-particle potential $U(k)$ defined by

$$U(k) = \sum_{k' \leq k_F} \text{Re} \langle kk' | G(e(k) + e(k')) | kk' \rangle_A \quad (3)$$

The G matrix is obtained by solving Eqs.(2,3) self-consistently, using the lattice QCD NN potential for V and the lattice QCD nucleon mass for M_N . Then the total energy E is obtained from Eq.(1). We employ the matrix inversion method [14] with the continuous choice for $U(k > k_F)$ [15]. Because of the limitation for the lattice QCD potentials available at present, we keep the partial-wave decomposition of the G -matrix only up to 1S_0 , 3S_1 , and 3D_1 channels.

Figure. 3 shows the ground state energy per nucleon (E/A) for the symmetric nuclear matter ($Z = N = A/2$ with the proton number Z , neutron number N and the

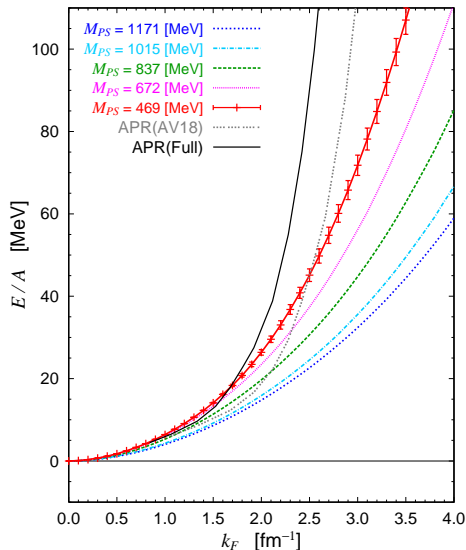


FIG. 4: Ground state energy per neutron for the pure neutron matter as a function of the Fermi momentum. Details of the calculation are the same as Fig. 3.

mass number $A = N + Z$) as a function of k_F for different m_q . The most important feature of the symmetric nuclear matter in the real world is its saturation property; i.e., E/A takes the minimum at normal nuclear matter density ρ_0 . The empirical saturation point from the Weizsäcker mass formula corresponds to $(k_F, E/A) \simeq (1.36 \text{ fm}^{-1}, -15.7 \text{ MeV})$ as indicated in Fig. 3. Also, we show the results of Ref. [16] which employs the variational method with AV18 NN potential with and without phenomenological three-nucleon NNN force.

Our result at the lightest quark mass ($M_{PS} \simeq 469 \text{ MeV}$) in Fig. 3 indicates that the symmetric nuclear matter becomes a self-bound system with a saturation point $(k_F, E/A) \simeq (1.83 \pm 0.16 \text{ fm}^{-1}, -5.4 \pm 0.5 \text{ MeV})$. Here the errors are statistical uncertainties estimated by dividing the gauge configurations into two sets. This is the first time that the nuclear force obtained from first principle lattice QCD simulations leads to the saturation in the symmetric nuclear matter. The saturation point, however, deviates from the empirical point primarily due to heavy quark masses in our lattice simulation and the lack of NNN force in our BHF calculation.

Also, we find nontrivial m_q dependence of the EOS: the saturation disappears at intermediate quark masses ($M_{PS} \simeq 672, 837 \text{ MeV}$) and appears again at the heavy quark mass region ($M_{PS} \simeq 1015, 1171 \text{ MeV}$). This implies that the saturation originates from a subtle balance between short-range repulsion and the intermediate attraction of the nuclear force which have different m_q dependence [9]. The saturation points for $M_{PS} \simeq 1015, 1171 \text{ MeV}$ locate at more than $10\rho_0$, so that the effect of finite lattice spacing and the validity of BHF theory need to

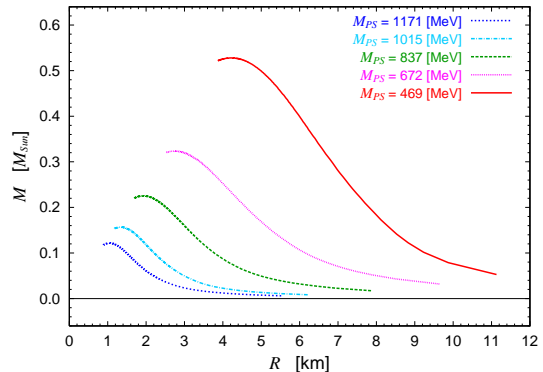


FIG. 5: Mass-radius relation of the neutron star. Neutron-star matter consists of n, p, e^- , and μ^- with charge neutrality and chemical equilibrium. EOS for the nucleons is obtained by an interpolation between Fig. 3 and Fig. 4 under the parabolic approximation.

be carefully checked for those cases. Our restriction of the NN interactions and the G matrix to the 1S_0 and 3S_1 - 3D_1 channels may not be a bad approximation, since the S wave is known to be a dominant contribution and higher partial waves tend to cancel with each other near the physical saturation point [17]. Nevertheless, we will include the results of on-going spin-orbit force calculation on the lattice [18] in the near future. In addition, we need to include the three-nucleon force from lattice QCD simulations [19] to make the EOS at high density more realistic.

Figure. 4 shows E/A for the pure neutron matter ($N = A$) as a function of k_F . In this case, neutron matter is not self-bound due to large Fermi energy. The pressure of the system is proportional to the slope of E/A as $P = \rho^2 \frac{\partial(E/A)}{\partial \rho} = \frac{k_F^4}{9\pi^2} \frac{\partial(E/A)}{\partial k_F}$; Fig. 4 indicates that P increases quite rapidly as m_q decreases.

To see the m_q dependence of the EOS for neutron-star matter, we calculate the mass (M) and the radius (R) of neutron stars for different m_q : The Tolman-Oppenheimer-Volkoff equation is solved by using the EOS of neutron-star matter with neutron, proton, electron and muon under the charge neutrality and beta equilibrium. For asymmetric nuclear matter, we use the parabolic approximation, $\frac{E}{A}(\rho, x) = \frac{E_{Z=N}}{A}(\rho) + (1 - 2x)^2 \epsilon_{\text{sym}}(\rho)$ with the symmetry energy $\epsilon_{\text{sym}} = E_{Z=0}/A - E_{Z=N}/A$ and the proton fraction $x = \rho_p/\rho$. This is a standard interpolation between the symmetric nuclear matter and pure neutron matter. The leptons (electrons and muons) are treated as the noninteracting Fermi gas. Solving the Tolman-Oppenheimer-Volkoff equation with a given value of central mass-energy density as an initial condition, we obtain the M - R relation for a spherically symmetric and nonrotating neutron star.

Shown in Fig. 5 is the M - R relation of the neutron star for different m_q . As m_q decreases, the M - R curve

shifts to the upper right direction, indicating directly the stiffening of our EOS. The maximum mass of the neutron star (M_{\max}) is found to be 0.53 times the solar mass (M_{\odot}) at the lightest m_q corresponding to $M_{\text{PS}} \simeq 469$ MeV and $M_N \simeq 1161$ MeV [20]. Such a maximum mass is too small to account for the observed neutron stars obviously due to the heavy m_q : A naive extrapolation of M_{\max} and the corresponding radius to $M_{\text{PS}} = 137$ MeV, with a function $f(M_{\text{PS}}) = a/(M_{\text{PS}} + b) + c$, for example, gives $M_{\max} = 2.2M_{\odot}$ and $R = 12$ km. Although this is a crude estimate, it is encouraging for future quantitative studies [21].

Throughout this Letter, the NN potentials are taken from the zero-strangeness sector of the octet-baryon potentials obtained by lattice QCD simulations with flavor- $SU(3)$ symmetry. In this case, the vacuum polarization of the s quark contributes equally to the u and d quarks, though the valence quarks are restricted to only u and d quarks in the NN sector. To be more realistic, we need to consider explicit breaking of flavor- $SU(3)$ symmetry: Studies along this line on the lattice have been already started [12] and results will be implemented in our future EOS calculation with the BHF theory.

To describe the nuclear matter and the neutron matter around the normal nuclear density, it is sufficient to focus on the zero-strangeness sector. However, as the density exceeds a few times the normal nuclear density, hyperons (Y) would start to appear in the ground state, which is particularly relevant to the central core of neutron stars (see e.g. [22] and references therein). Therefore, construction of the EOS with YN and YY interactions is an important next step in our approach. Since the hyperon forces are not well constrained by the experimental data, the results of the lattice QCD simulations [12] are quite useful. The three-baryon interactions [19] with hyperons will also be important to construct a realistic EOS to sustain recently discovered massive neutron stars. The results of the present Letter provide a starting point of all these developments in the near future.

We thank K.-I. Ishikawa and the PACS-CS group for providing their DDHMC/PHMC code [23], and authors and maintainer of CPS++ [24], whose modified version is used in this Letter. Numerical computations of this work have been carried out at Univ. of Tsukuba super-computer system (T2K). This research is supported in part by Grant-in-Aid for Scientific Research on Innovative Areas(No.2004:20105001, 20105003) and for Scientific Research (B) 25287046, 24740146, (C) 23540321 and SPIRE (Strategic Program for Innovative REsearch). T.H. was partially supported by RIKEN iTHES Project.

- (2010); J. Antoniadis, *et al.*, Science **340**, 6131 (2013)
- [2] Y. Sekiguchi, K. Kiuchi, K. Kyutoku, and M. Shibata, Phys. Rev. Lett. **107**, 051102 (2011)
- [3] H.-T. Janka, F. Hanke, L. Huedepohl, A. Marek, B. Mueller, and M. Obergaulinger, Prog. Theor. Phys. **2012**, 01A309 (2012)
- [4] M. Baldo and G.F. Burgio, Rept. Prog. Phys. **75**, 026301 (2012)
- [5] J. Carlson, S. Gandolfi, and A. Gezerlis, Prog. Theor. Exp. Phys. **2012**, 01A209 (2012)
- [6] K. Hebeler, J.M. Lattimer, C.J. Pethick, and A. Schwenk, Astrophys. J. **773**, 11 (2013)
- [7] J.W. Holt, N. Kaiser and W. Weise, arXiv:1304.6350
- [8] T. Inoue, N. Ishii, S. Aoki, T. Doi, T. Hatsuda, Y. Ikeda, K. Murano, H. Nemura, and K. Sasaki (HAL QCD Collaboration), Phys. Rev. Lett. **106**, 162002 (2011)
- [9] T. Inoue, S. Aoki, T. Doi, T. Hatsuda, Y. Ikeda, N. Ishii, K. Murano, H. Nemura, and K. Sasaki (HAL QCD Collaboration), Nucl. Phys. A **881**, 28 (2012)
- [10] N. Ishii, S. Aoki, and T. Hatsuda, Phys. Rev. Lett. **99**, 022001 (2007) S. Aoki, T. Hatsuda and N. Ishii, Prog. Theor. Phys. **123**, 89 (2010)
- [11] N. Ishii, S. Aoki, T. Doi, T. Hatsuda, Y. Ikeda, T. Inoue, K. Murano, H. Nemura, and K. Sasaki (HAL QCD Collaboration), Phys. Lett. **B712** (2012) 437.
- [12] S. Aoki, T. Doi, T. Hatsuda, Y. Ikeda, T. Inoue, N. Ishii, K. Murano, H. Nemura, and K. Sasaki (HAL QCD Collaboration), Prog. Theor. Exp. Phys. **2012**, 01A105 (2012)
- [13] We note that the absence of the bound deuteron at $M_{\text{PS}} \simeq 469\text{MeV}$ found in the HAL QCD method is in contrast to the results using the Lüscher's method, although simulation parameters are somewhat different: T. Yamazaki, K.-I. Ishikawa, Y. Kuramashi and A. Ukawa, Phys. Rev. D **86**, 074514 (2012) S.R. Beane, E. Chang, W. Detmold, H.W. Lin, T.C. Luu, K. Orginos, A. Parreño, M. J. Savage, A. Torok, and A. Walker-Loud (NPLQCD Collaboration), Phys. Rev. D **85**, 054511 (2012)
- [14] M.I. Haftel and F. Tabakin, Nucl. Phys. **A158**, 1 (1970)
- [15] H.Q. Song, M. Baldo, G. Giansiracusa, and U. Lombardo, Phys. Rev. Lett. **81**, 1584 (1998).
- [16] A. Akmal, V.R. Pandharipande and D. G. Ravenhall, Phys. Rev. C **58**, 1804 (1998)
- [17] M. Baldo, I. Bombaci, L.S. Ferreira, G. Giansiracusa, and U. Lombardo, Phys. Rev. C **43**, 2605 (1991).
- [18] K. Murano, N. Ishii, S. Aoki, T. Doi, T. Hatsuda, Y. Ikeda, T. Inoue, H. Nemura, and K. Sasaki (HAL QCD Collaboration), arXiv:1305.2293.
- [19] T. Doi, S. Aoki, T. Hatsuda, Y. Ikeda, T. Inoue, N. Ishii, K. Murano, H. Nemura, and K. Sasaki (HAL QCD Collaboration), Prog. Theor. Phys. **127**, 723 (2012)
- [20] E/A and its slope for $M_{\text{PS}}=469\text{MeV}$ in Fig.4 is already rather close to APR for $k_F < 1.5 \text{ fm}^{-1}$. This implies that small M neutron star with the central density not far from ρ_0 have a radius of about 10 km. This is actually seen in Fig.5.
- [21] The crust EOS, which is unknown for unphysical m_q and thus is not included in our calculation, would increase R for small M without affecting M_{\max} . We checked this qualitatively by matching our EOS with the Baym-Pethick-Sutherland (BPS) EOS taken from Table 7 of [6].
- [22] K. Masuda, T. Hatsuda and T. Takatsuka, Astrophys. J. **764**, 12 (2013)

[1] P. Demorest, T. Pennucci, S.M. Ransom, M.S.E. Roberts, and J.W.T. Hessels, Nature (London) **467**, 1081

[23] S. Aoki *et al.* [PACS-CS Coll.], Phys. Rev. D **79**, 034503 (2009)

[24] Columbia Physics System (CPS),

<http://qcdoc.phys.columbia.edu/cps.html>